Published in final edited form as:
NMR Biomed. 2013 January ; 26(1): 51–57. doi:10.1002/nbm.2818.

Feasibility of Measuring Prostate Perfusion with Arterial Spin Labeling

Xiufeng Li and **Gregory J. Metzger***
Center for Magnetic Resonance Research, Radiology, University of Minnesota, MN, United States

Abstract

Prostate perfusion has the potential to be an important pathophysiological marker for monitoring disease progression or assessing therapeutic response of prostate cancer. The feasibility of arterial spin labeling (ASL), an MRI approach for measuring perfusion without an exogenous contrast agent, is demonstrated in the prostate for the first time. While various ASL methods have been previously demonstrated in highly perfused organs such as the brain and kidneys, the prospect of obtaining such measurements in the prostate is challenging due to relatively low blood flow, long transit times, susceptibility induced image distortion and local motion. However, despite these challenges, this study demonstrates that with a whole body transmit coil and external receiver array, global prostate perfusion can be measured with ASL at 3T. In five healthy subjects with a mean age of 44 years, the mean total prostate blood flow (PBF) was measured to be 25.8 ± 7.1 mL/100 cm^3/min, with an estimated bolus duration and arterial transit time of 884 ± 209 ms and 721 ± 131 ms, respectively.

Keywords

perfusion; blood flow; arterial spin labeling (ASL); FAIR; prostate; prostate blood flow (PBF)

INTRODUCTION

Prostate cancer is the most common malignancy and the second leading cause of death for men in the United States (1). Early tumor growth is strongly associated with angiogenesis (2), a key pathophysiological characteristic associated with tumor grade and metastatic potential (3,4). Angiogenesis results in the development of vessels and elevated blood supply to support tumor growth. Therefore, to the ability to measure prostate blood flow (PBF) has the potential to improve early diagnosis (5), assess disease aggressiveness and monitor disease progression. Meanwhile, a wide variety of antiangiogenic drugs have been developed and used as treatment options for prostate cancer (6–8). These drugs can suppress tumor angiogenesis or destroy tumor vasculature, resulting in decreased blood flow. PBF may be an important biomarker for monitoring the efficacy of these and other therapeutic interventions (9).

There are several imaging techniques available for determining prostate perfusion including ^{15}O-PET (positron emission tomography) (5), dynamic contrast-enhanced magnetic resonance imaging (DCE-MRI) (10,11) and arterial spin labeling (ASL).

*Presented in part at the 19th ISMRM in Montreal, Québec, Canada, 2011.

Address correspondence: Greg Metzger, Ph.D., The University of Minnesota, 2021 Sixth Street SE, Minneapolis, MN 55455, Tel: 612-626-2001, FAX: 612-626-2004, gmetzger@umn.edu.

Compared to other perfusion imaging modalities, ASL (12–14) is non-invasive as it does not require the use of an exogenous contrast agent, making it a potentially useful tool in the longitudinal monitoring of tumor progression or treatment (9). Previous applications of ASL in the study of cancer have shown successful use in evaluating tumor angiogenesis and assessing grade in both the brain and highly perfused peripheral organs (15–19).

The purpose of this study was to evaluate the feasibility of performing ASL prostate perfusion imaging with a surface array receive coil at 3T. The main challenge of using ASL in the prostate is intrinsically low signal to noise ratio which is exacerbated by the relatively slow blood flow to the prostate from multiple feeding vessels (20). To our knowledge, this is the first demonstration of using ASL to study perfusion in the human prostate.

METHODS

Subject

Five healthy male adults, ages 44 ± 16 years (mean ± standard deviation), participated in an institutional review board approved protocol, involving a multiple inversion ASL perfusion study. Written informed consent was obtained from each participant.

MRI Scanner and FAIR Sequence

All studies were performed on a 3T Siemens TIM Trio, transmitting with the whole body coil and receiving with combined surface array (two rows of 3 elements) anteriorly and the spine array (two rows of 3 elements) posteriorly.

All perfusion studies used a modified spatially-confined FAIR sequence (21). The sequence diagram and the location of the inversion and imaging slabs are illustrated in Figures 1a and 1b, respectively. In the labeling portion of the sequence, a weaker slice selective gradient was used to invert a 230 mm slab, referred to as the spatially-confined inversion slab. In the control portion of the sequence, a stronger slice selective gradient was applied for the inversion of a 50 mm slab covering the imaging volume, referred to as the imaging section inversion slab (Figure 1a). The inversion RF pulse for tagging was a hyperbolic secant pulse with a duration of 15.36 ms, amplitude of 22 μT and a labeling efficiency of 95%. The gradient amplitude for a 100 mm inversion slab was 0.7 mT/m (22). In both labeling and control acquisitions, one pre-inversion and two post-inversion saturations were performed over the imaging section inversion slab to minimize the subtraction error due to a non-ideal inversion profile. After a user-specified delay time (TI), images were acquired with an echo planar imaging (EPI) readout with a real-time prospective motion correction technique to reduce large bulk subject motion effects (23).

ASL Prostate Perfusion Study

The blood supply for the prostate originates primarily from four arteries: inferior vesical, middle rectal, internal pudental and inferior gluteal arteries, all of which are the branches of internal iliac artery (20). Therefore, the labeling site for ASL imaging is the superior/posterior region of the prostate (Figure 1b). Imaging slices were consistently positioned perpendicular to the rectal wall for all subjects with the most superior slice covering the base of the prostate.

After a multi-planar scout imaging series and before the multi-inversion ASL perfusion imaging, anatomic T2-weighted images were acquired in the axial, sagittal and coronal planes using a turbo spin echo (TSE) acquisition to assist ASL positioning (TR/TE = 6000/11 ms, resolution = 0.86 × 0.86 × 3 mm^3, flip angle = 140°).

The multiple inversion perfusion studies consisted of five different inversion times: 0.7, 1.0, 1.3, 1.6, and 2.0 s, the order of which was randomized for each subject. Imaging parameters for the ASL acquisition included: TR/TE = 3000/9 ms, FOV = 220 × 220 mm^2, matrix size = 64 × 64, in-plane imaging resolution = 3.44 × 3.44 mm^2, slice thickness/gap = 5.0/1.0 mm, number of slices = 5, phase oversampling = 10% with A-P direction, acquisition order = descending, GRAPPA iPAT factor = 2 with 24 reference lines, partial Fourier = 7/8, selective inversion slab = 50 mm and a spatially-confined inversion slab = 230 mm. Volumetric, static B0 shimming was performed over the entire imaging slab. Proton density images (M_0) were also acquired by using the same EPI imaging parameters but with a longer TR (8 s). For all ASL perfusion imaging studies, no intensity normalization correction was performed to avoid changing background noise levels or imaging contrast which could affect the following error analysis.

During each study, acquired imaging volumes were visually inspected in movie play mode on the console of the scanner to observe how often local motion occurred in the prostate region. To compensate the adverse effects of local motion on EPI image quality, more volumes were acquired for each inversion time in subjects in which more frequent motion was observed. Across subjects, the number of acquired EPI volumes for each inversion time ranged from 240 to 300, resulting in acquisition times between 12 to 15 min.

At the end of the perfusion scans, anatomic T2-weighted images were acquired matching the ASL perfusion imaging series in terms of slice thickness, position and orientation using a TSE sequence (TR/TE = 2030/119 ms, resolution = 0.86 × 0.86 × 5 mm^3, slice gap = 1 mm, number of imaging slices = 5, flip angle = 120°). These anatomic images were used as the reference for prostate ROI definition.

Imaging processing and Data Analysis

Post-processing of the ASL data was performed using SPM 2 (Functional Imaging Laboratory, University College London) including both motion correction between volumes and co-registration of the ASL data with the reference anatomic images. Iterative non-linear least squares model fitting was performed in Matlab 7.1 (The MathWorks, Inc., Natick, Massachusetts) for measured perfusion signals from the multiple inversion time experiment.

Image Pre-processing—All ASL imaging series were first evaluated for subject bulk motion. Pairs of labeled and control images with sudden and/or large motions (>0.5 mm translation and 0.5 degree rotation) were excluded from data analysis. For some imaging series, there existed small but continuous translations and/or rotations throughout the acquisition of a series, resulting in relatively large accumulated differences between images at the beginning of the series and those at the end. Such imaging series were co-registered to further minimize the effects of motion on the perfusion calculations. At last, a final visual inspection was performed to remove those pairs of label/control images with obvious local prostate motion. The number of discarded pairs of label/control images varied from subject to subject, ranging from 8% to 15% of total label/control pairs. To be consistent, a total of 110 pairs of label/control images were used in the final analysis for all subjects by excluding any extra volumes from the end of each time series.

Each ASL label-control image series was pair-wise subtracted to obtain a perfusion-weighted imaging series which was further averaged across subtracted pairs of a given inversion experiment to produce a mean perfusion weighted image.

Iterative Model-fitting—Iterative non-linear least squares model-fitting was performed in MatLab 7.0 to fit the mean perfusion signal versus inversion time to a three-phase, single blood compartment model (24):

$$\Delta M(t)=0 \quad 0<t<\Delta t \quad [1]$$

$$=2M_0 f(t-\Delta t)\exp(-t/T_{1b}) \quad \Delta t<t<\tau+\Delta t \quad [2]$$

$$=2M_0 f\tau\exp(-t/T_{1b}) \quad \tau+\Delta t<t \quad [3]$$

where ΔM(t) is the measured mean perfusion signal in specified ROIs surrounding the prostate at inversion time t, Δt the transit time, τthe bolus duration, f prostate blood flow (PBF), M_0 the fully relaxed magnetization of the prostate tissue and T_{1b} the longitudinal relaxation time of the arterial blood which was assumed 1660 ms (25). By using a single blood compartment model, the clearance of labeling blood bolus via venous outflow was not considered.

To avoid the adverse effects of labeled blood signal from larger arteries and subtraction errors due to small residual motion, trimmed mean ASL signals were used for ASL model fitting, by excluding the 5% of voxels with the lowest values and the 5% with the highest values for measured perfusion signals at each inversion time (26). Due to the fact that this was a multi-slice acquisition, the slice dependent longitudinal decay of the perfusion signal was compensated for prior to signal averaging and model fitting (27).

Measurement Error Analysis—Error propagation analysis was performed to evaluate the measurement error due to random (white) noise (σ_{random}), or temporal (physiological) noise ($\sigma_{temporal}$) by using an approach previously presented in the literature (28):

$$E_{random}=\frac{\sigma_{random}\sqrt{2/N_{voxel}}}{(2M_0\tau\exp(-TI/T_{1b}))} \quad [4]$$

$$E_{temporal}=\sigma_{temporal}/\sqrt{N_{PWI}} \quad [5]$$

where E_{random} and $E_{temporal}$ represent random an d temporal measurement errors respectively, N_{voxel} represents the total number of averaged voxels, N_{PWI} the number of averaged perfusion weighted images, τ the assumed temporal bolus duration of labeled blood, and TI the inversion time. The random noise σ_{random} was estimated from 50 background voxels and the temporal noise $\sigma_{temporal}$ was estimated by using the standard deviation over time of the measured mean perfusion signals in the prostate.

Random and temporal errors were calculated and evaluated as the percentage of estimated PBF for each subject by using measurements at delay times of 1.6 s with an assumed bolus duration 0.8 s. The estimations of PBF using measurements from a single inversion time used the following simplified single blood compartment model (29):

$$f=\Delta M/(2M_0\tau\exp(-TI/T_{1b})) \quad [6]$$

where ΔM represents the measured ASL difference signal between labeling and control images in specified ROIs at inversion time TI, and the other parameters are as defined in equation 1–5.

Data Analysis—The distortion of the EPI ASL images induced by residual B_0 inhomogeneity can result in poor co-registration with the T2-weighted images. Therefore, the regions of interests (ROIs) were manually drawn using the proton density images

acquired with the same EPI readout while using the T2-weighted images as a reference. The manually drawn ROIs were defined conservatively to ensure that they were within the prostate, covering both peripheral and central zones. Mean perfusion signals within these defined ROIs were obtained for each subject.

RESULTS

Perfusion results from one subject are presented in Figures 2a and 2b. The perfusion-weighted imaging maps of a single slice near the center of the prostate are displayed for the other four subjects in Figure 3. The group mean ASL signal changes with inversion time are shown in Figure 4a after compensating for relaxation decay, and the estimated arterial transit time and temporal bolus width are presented in Figure 4b.

The mean PBF estimated by using a single inversion time measurement of 1.6 s was 25.8 ± 7.1 mL/100 cm^3/min (mean±standard deviation). For each subject, estimated measurement errors due to random and temporal noise, as well as subject age and prostate volume, are presented in Table 1. The estimated measurement errors due to random/thermal noise are quite small, less than 10% for all subjects. In contrast, temporal/physiological errors are much higher than random errors, and can be as high as 36.6% of the estimated PBF. Therefore the major source of measurement error arises from the temporal and not random sources.

DISCUSSION

For the first time, the feasibility of measuring prostate perfusion using ASL has been demonstrated. The measured signal changes with inversion time reflected the inflow of labeled blood into prostate tissue where an initial signal increase with increasing inversion time was followed by signal decreases at later inversion times. As an important index of tissue viability, tissue perfusion has the potential assist in the diagnosis and prognosis of prostate cancer. As a non-invasive and non-radioactive approach, ASL is suitable for the longitudinal monitoring of vascular/perfusion changes associated with disease progression or therapeutic response.

Based on the fact that the longitudinal relaxation time of prostate tissue (1597±42 ms) (30) is very close to that of arterial blood (25), a single blood compartment model was selected for both iterative nonlinear least squares model fitting of the multi-inversion data and PBF quantification using a single inversion time measurement. To improve the results obtained with this model, several sequence timing parameters were also optimized. The effect of T2* on PBF quantification was minimized by using both parallel imaging and partial Fourier to reduce the TE to as short as 9 ms (31). Meanwhile, to ensure that there was sufficient refreshment of the fast inflowing blood in big upstream arteries within the labeling region, a TR of 3 s was used. It should be noted that arterial transit times can be shortened due to tumor angiogenesis (11), and may change during longitudinal monitoring of therapy. When using the FAIR technique in prostate cancer studies, these potential variations in transit time should be considered to avoid either overestimation or underestimation of prostate blood flow.

The results of this study indicate that compared to the brain or other organs, such as the kidney, blood flow in the prostate is quite low, and transit times are considerably longer. Despite these challenges, estimates of overall prostate blood flow determined with ASL are comparable with those in the literature when using either contrast enhanced MRI (23 ± 21 mL/100 cm^3/min (11) and 32 ± 36 mL/100 cm^3/min (10)) or ^{15}O-PET (15.7 ± 7.5 mL/100 cm^3/min (5)).

Although prostate perfusion quantification is not the major focus of this paper, the performed studies provide valuable information that can guide the selection/optimization of ASL parameters for future quantification studies. To simplify PBF quantification and improve quantification accuracy, a single-subtraction quantification method, such as Q2TIPS (32), could be applied in the future. Based on the estimated arterial transit time and temporal bolus width determined in this study, the Q2TIPS method could be employed using a labeling time of approximately 0.7 s and a relatively long post-bolus delay time of 0.8 s. Without considering limitations in SNR, an even longer post-bolus delay time would be preferred to avoid intravascular artifacts. To further improve quantification, a prostate specific tissue-blood partition coefficient could be measured and used as well in future studies. In its absence, the fully relaxed magnetization of the prostate was used for quantification in this study.

Our initial experience of performing ASL studies to measure prostate perfusion indicates that it is challenging to get high quality and reliable results not only because of low perfusion and long transit times, but also because of the following issues: 1) surface arrays, such as those used in this study, have low SNR in the prostate; 2) variable susceptibility near the rectal wall due to the presence of gas results in geometric distortions and signal loss even when parallel imaging and short echo times have been used; and 3) local prostate/rectal motion, which can generate substantial subtraction errors, results in large temporal measurement errors. In the current study, to address the issue of motion, increasing numbers of volumes were acquired in the presence of greater prostate motion to provide a sufficient number of volumes for averaging after rejection. The need to discard data reduces the chances that sufficient averages could be obtained to significantly increase the SNR beyond that presented with the current methods and coils. Therefore, it is unlikely that data suitable for sub-region analysis of the prostate, necessary for quantifying anything other than global prostate perfusion, could be obtained unless modifications to the methods are implemented.

Some of the challenges detailed above may be addressed by using an endorectal coil (ERC) which has significantly higher SNR than surface arrays, potentially decreases local prostate motion and, when inflated with susceptibility matching fluids, reduces B_0 induced distortions (33,34). The increased SNR may also make it possible to obtain sub-region measures of perfusion. A potential disadvantage of the ERC coil is that the inhomogeneous sensitivity profile may result in increased temporal errors induced by residual local motion.

Improvements in the acquisition and post-processing methods may also benefit prostate ASL perfusion studies. The use of other imaging readout methods, such as true fast imaging with steady state precession (TrueFISP) and turbo spin echo (TSE), and the application of non-rigid co-registration in post-imaging processing can also help improve imaging quality and therefore the reliability of PBF quantification. All of these options are currently under investigation.

This study shows a relatively large inter-subject variability in the estimated arterial transit time, temporal bolus, PBF and measurement errors. In addition to the relatively low SNR of these acquisitions, the variability could result from the large range of subject ages, subject-dependent local motion, and possibly from variations in subject-dependent vascular geometry (20). For example, considerably lower prostate perfusion was obtained for one subject exhibiting only modest motion between volumes during the perfusion acquisition. The low perfusion in this case may, primarily, be a result of subject-dependent vascular geometry, the influence of which requires further study.

CONCLUSION

The preliminary data in this study indicates that prostate perfusion can be measured with ASL; however, further technical developments and studies are required to improve imaging quality and reduce the sources of variability in the determined PBF before ASL prostate perfusion imaging method can be applied clinically.

Acknowledgments

This project was supported by the National Cancer Institute (R01-CA131013), National Center for Research Resources (P41 RR008079) and the National Institute of Biomedical Imaging and Bioengineering (P41 EB015894). The authors would also like to acknowledge Victoria Vescovo Webster, MA, (Medical Illustrator, Center for Genetics of Host Defense, UT Southwestern Medical Center, Dallas, TX) for her help in the preparation of the vascular anatomy illustration.

Abbreviations used

ASL	arterial spin labeling
PBF	prostate blood flow
FAIR	flow-sensitive alternating inversion recovery
Q2TIPS	QUIPSS II with thin-slice TI1 periodic saturation
EPI	echo planar imaging
ROI	region of interest
SNR	signal-to-noise ratio
DCE	dynamic contrast enhanced
TSE	turbo spin echo
TrueFISP	true fast imaging with steady state precession
ERC	endorectal coil
PET	positron emission tomography

REFERENCES

1. Siegel R, Ward E, Brawley O, Jemal A. Cancer statistics, 2011: The impact of eliminating socioeconomic and racial disparities on premature cancer deaths. CA Cancer J Clin.
2. Folkman J, Watson K, Ingber D, Hanahan D. Induction of angiogenesis during the transition from hyperplasia to neoplasia. Nature. 1989; 339(6219):58–61. [PubMed: 2469964]
3. Folkman J. Role of angiogenesis in tumor growth and metastasis. Semin Oncol. 2002; 29(6 Suppl 16):15–18. [PubMed: 12516034]
4. Brawer MK, Deering RE, Brown M, Preston SD, Bigler SA. Predictors of Pathological Stage in Prostatic-Carcinoma - the Role of Neovascularity. Cancer. 1994; 73(3):678–687. [PubMed: 7507798]
5. Inaba T. Quantitative measurements of prostatic blood flow and blood volume by positron emission tomography. J Urol. 1992; 148(5):1457–1460. [PubMed: 1279212]
6. Dahut WL, Gulley JL, Arlen PM, Liu Y, Fedenko KM, Steinberg SM, Wright JJ, Parnes H, Chen CC, Jones E, Parker CE, Linehan WM, Figg WD. Randomized phase II trial of docetaxel plus thalidomide in androgen-independent prostate cancer. Journal of clinical oncology : official journal of the American Society of Clinical Oncology. 2004; 22(13):2532–2539. [PubMed: 15226321]
7. Nemunaitis J, Poole C, Primrose J, Rosemurgy A, Malfetano J, Brown P, Berrington A, Cornish A, Lynch K, Rasmussen H, Kerr D, Cox D, Millar A. Combined analysis of studies of the effects of the matrix metalloproteinase inhibitor marimastat on serum tumor markers in advanced cancer:

selection of a biologically active and tolerable dose for longer-term studies. Clinical cancer research : an official journal of the American Association for Cancer Research. 1998; 4(5):1101–1109. [PubMed: 9607566]

8. Steinbild S, Mross K, Frost A, Morant R, Gillessen S, Dittrich C, Strumberg D, Hochhaus A, Hanauske AR, Edler L, Burkholder I, Scheulen M. A clinical phase II study with sorafenib in patients with progressive hormone-refractory prostate cancer: a study of the CESAR Central European Society for Anticancer Drug Research-EWIV. British journal of cancer. 2007; 97(11): 1480–1485. [PubMed: 18040273]
9. Ludemann L, Wust P, Gellermann J. Perfusion measurement using DCE-MRI: implications for hyperthermia. Int J Hyperthermia. 2008; 24(1):91–96. [PubMed: 18214772]
10. Buckley DL, Roberts C, Parker GJ, Logue JP, Hutchinson CE. Prostate cancer: evaluation of vascular characteristics with dynamic contrast-enhanced T1-weighted MR imaging--initial experience. Radiology. 2004; 233(3):709–715. [PubMed: 15498903]
11. Ludemann L, Prochnow D, Rohlfing T, Franiel T, Warmuth C, Taupitz M, Rehbein H, Beyersdorff D. Simultaneous quantification of perfusion and permeability in the prostate using dynamic contrast-enhanced magnetic resonance imaging with an inversion-prepared dual-contrast sequence. Ann Biomed Eng. 2009; 37(4):749–762. [PubMed: 19169821]
12. Kim SG, Tsekos NV. Perfusion imaging by a flow-sensitive alternating inversion recovery (FAIR) technique: application to functional brain imaging. Magn Reson Med. 1997; 37(3):425–435. [PubMed: 9055234]
13. Wong EC. Quantifying CBF with pulsed ASL: technical and pulse sequence factors. Journal of magnetic resonance imaging : JMRI. 2005; 22(6):727–731. [PubMed: 16261572]
14. Wu WC, Fernandez-Seara M, Detre JA, Wehrli FW, Wang J. A theoretical and experimental investigation of the tagging efficiency of pseudocontinuous arterial spin labeling. Magn Reson Med. 2007; 58(5):1020–1027. [PubMed: 17969096]
15. Gaa J, Warach S, Wen P, Thangaraj V, Wielopolski P, Edelman RR. Noninvasive perfusion imaging of human brain tumors with EPISTAR. Eur Radiol. 1996; 6(4):518–522. [PubMed: 8798035]
16. Silva AC, Kim SG, Garwood M. Imaging blood flow in brain tumors using arterial spin labeling. Magn Reson Med. 2000; 44(2):169–173. [PubMed: 10918313]
17. Kimura H, Takeuchi H, Koshimoto Y, Arishima H, Uematsu H, Kawamura Y, Kubota T, Itoh H. Perfusion imaging of meningioma by using continuous arterial spin-labeling: comparison with dynamic susceptibility-weighted contrast-enhanced MR images and histopathologic features. AJNR Am J Neuroradiol. 2006; 27(1):85–93. [PubMed: 16418363]
18. Wolf RL, Wang J, Wang S, Melhem ER, O'Rourke DM, Judy KD, Detre JA. Grading of CNS neoplasms using continuous arterial spin labeled perfusion MR imaging at 3 Tesla. Journal of magnetic resonance imaging : JMRI. 2005; 22(4):475–482. [PubMed: 16161080]
19. De Bazelaire C, Rofsky NM, Duhamel G, Michaelson MD, George D, Alsop DC. Arterial spin labeling blood flow magnetic resonance imaging for the characterization of metastatic renal cell carcinoma(1). Acad Radiol. 2005; 12(3):347–357. [PubMed: 15766695]
20. Clegg EJ. The arterial supply of the human prostate and seminal vesicles. J Anat. 1955; 89(2):209–216. [PubMed: 14367216]
21. Zhang Y, Song HK, Wang J, Techawiboonwong A, Wehrli FW. Spatially-confined arterial spin-labeling with FAIR. Journal of magnetic resonance imaging : JMRI. 2005; 22(1):119–124. [PubMed: 15971191]
22. Wang J, Licht DJ, Jahng GH, Liu CS, Rubin JT, Haselgrove J, Zimmerman RA, Detre JA. Pediatric perfusion imaging using pulsed arterial spin labeling. Journal of magnetic resonance imaging : JMRI. 2003; 18(4):404–413. [PubMed: 14508776]
23. Thesen S, Heid O, Mueller E, Schad LR. Prospective acquisition correction for head motion with image-based tracking for real-time fMRI. Magn Reson Med. 2000; 44(3):457–465. [PubMed: 10975899]
24. Buxton RB, Frank LR, Wong EC, Siewert B, Warach S, Edelman RR. A general kinetic model for quantitative perfusion imaging with arterial spin labeling. Magn Reson Med. 1998; 40(3):383–396. [PubMed: 9727941]

25. Lu H, Clingman C, Golay X, van Zijl PC. Determining the longitudinal relaxation time (T1) of blood at 3.0 Tesla. Magn Reson Med. 2004; 52(3):679–682. [PubMed: 15334591]

26. MacIntosh BJ, Pattinson KT, Gallichan D, Ahmad I, Miller KL, Feinberg DA, Wise RG, Jezzard P. Measuring the effects of remifentanil on cerebral blood flow and arterial arrival time using 3D GRASE MRI with pulsed arterial spin labelling. Journal of cerebral blood flow and metabolism : official journal of the International Society of Cerebral Blood Flow and Metabolism. 2008; 28(8): 1514–1522. [PubMed: 18506198]

27. Yang Y, Frank JA, Hou L, Ye FQ, McLaughlin AC, Duyn JH. Multislice imaging of quantitative cerebral perfusion with pulsed arterial spin labeling. Magn Reson Med. 1998; 39(5):825–832. [PubMed: 9581614]

28. Zun Z, Wong EC, Nayak KS. Assessment of myocardial blood flow (MBF) in humans using arterial spin labeling (ASL): feasibility and noise analysis. Magn Reson Med. 2009; 62(4):975–983. [PubMed: 19672944]

29. Buxton RB. Quantifying CBF with arterial spin labeling. Journal of magnetic resonance imaging : JMRI. 2005; 22(6):723–726. [PubMed: 16261574]

30. de Bazelaire CM, Duhamel GD, Rofsky NM, Alsop DC. MR imaging relaxation times of abdominal and pelvic tissues measured in vivo at 3.0 T: preliminary results. Radiology. 2004; 230(3):652–659. [PubMed: 14990831]

31. St Lawrence KS, Wang J. Effects of the apparent transverse relaxation time on cerebral blood flow measurements obtained by arterial spin labeling. Magn Reson Med. 2005; 53(2):425–433. [PubMed: 15678532]

32. Luh WM, Wong EC, Bandettini PA, Hyde JS. QUIPSS II with thin-slice TI1 periodic saturation: a method for improving accuracy of quantitative perfusion imaging using pulsed arterial spin labeling. Magn Reson Med. 1999; 41(6):1246–1254. [PubMed: 10371458]

33. Noworolski SM, Crane JC, Vigneron DB, Kurhanewicz J. A clinical comparison of rigid and inflatable endorectal-coil probes for MRI and 3D MR spectroscopic imaging (MRSI) of the prostate. Journal of magnetic resonance imaging : JMRI. 2008; 27(5):1077–1082. [PubMed: 18407539]

34. Rosen Y, Bloch BN, Lenkinski RE, Greenman RL, Marquis RP, Rofsky NM. 3T MR of the prostate: reducing susceptibility gradients by inflating the endorectal coil with a barium sulfate suspension. Magn Reson Med. 2007; 57(5):898–904. [PubMed: 17457870]

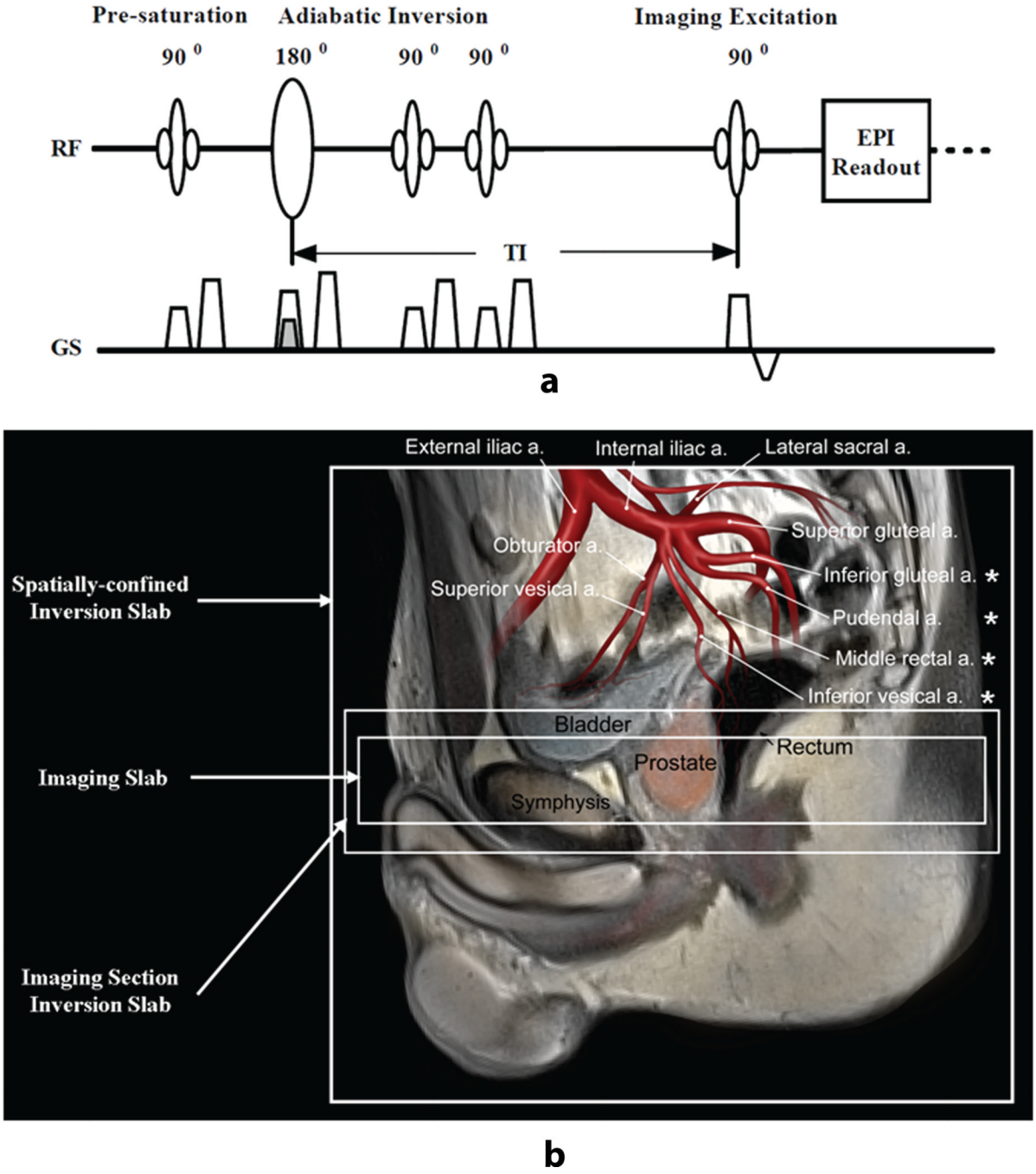

Figure 1.

(a) ASL sequence diagram for labeling and control imaging acquisition, (b) the spatial definition and planning of slabs used for spatially-confined inversion, imaging section inversion, and imaging. The stronger gradient for the imaging section inversion (control) and the weaker gradient for the spatially-confined inversion (labeling) are superposed on the sequence diagram. The arrangement of the slabs relative to feeding arteries in the superior region of the prostate is overlaid on the anatomic T2-weighted image. The four major arteries supplying blood to the prostate are indicated by asterisks (*). The ‘a.’ in (b) is an abbreviation for artery.

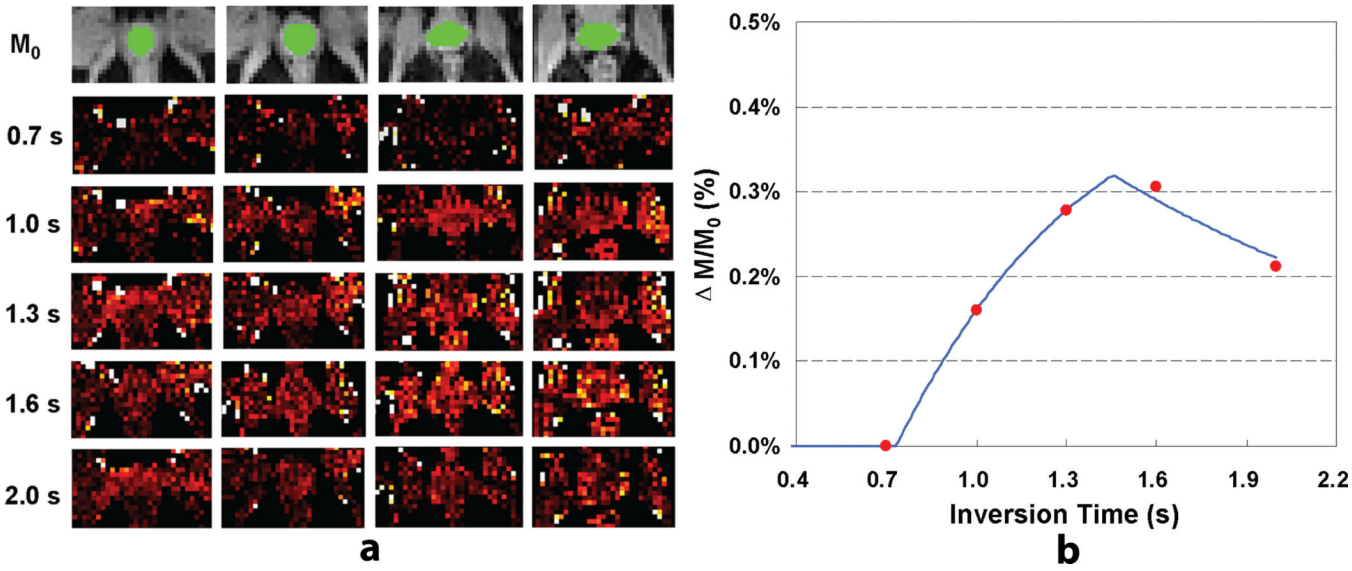

Figure 2.
Prostate perfusion imaging results from one subject: (a) proton density images with overlaid ROIs (top row) and perfusion-weighted imaging maps acquired at different delay times from one subject; (b) a plot of ASL signal changes as a function of delay time and the corresponding model fitting curve.

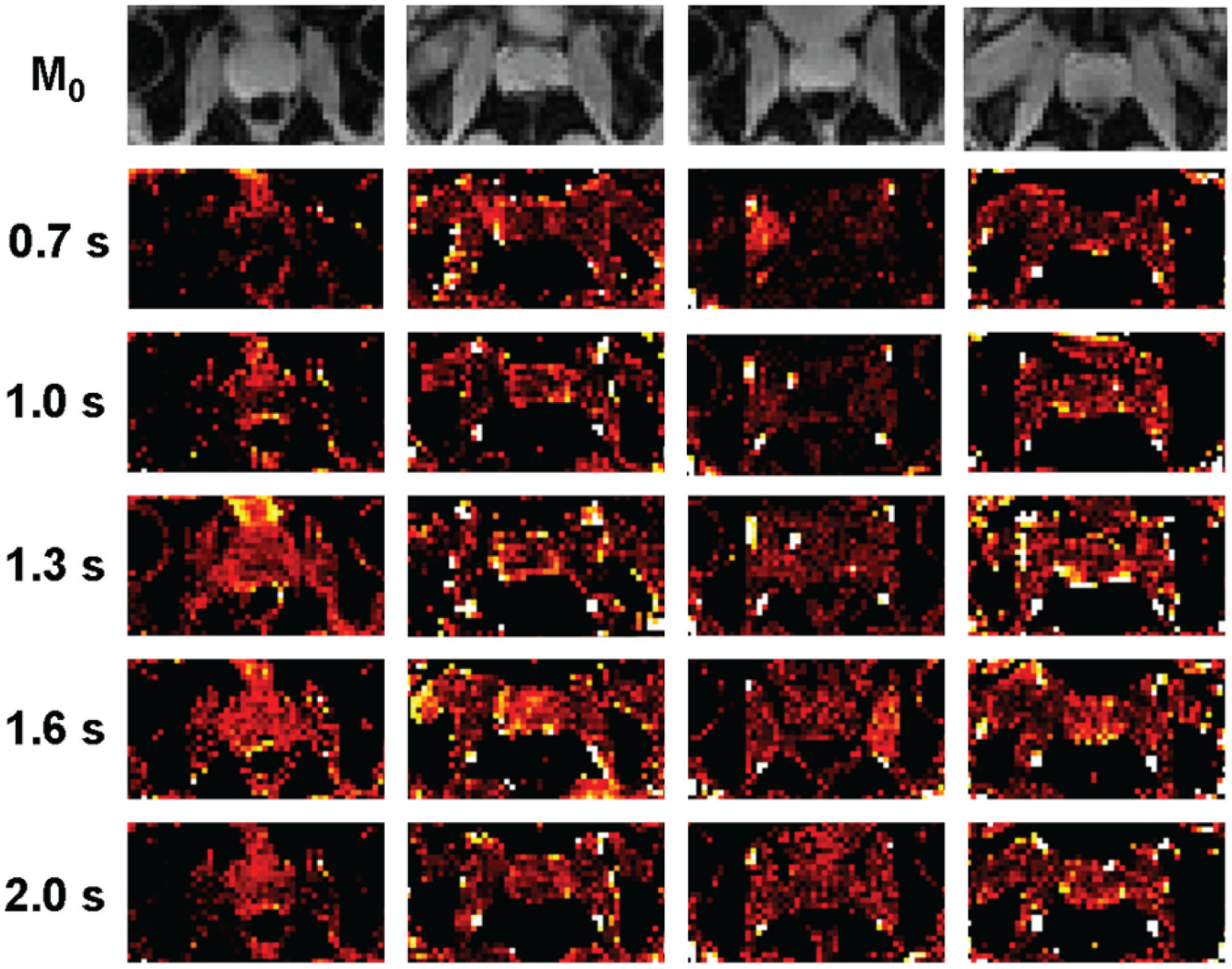

Figure 3.
Proton density images and perfusion-weighted imaging maps of a single slice near the center of the prostate for the other four subjects included in this study.

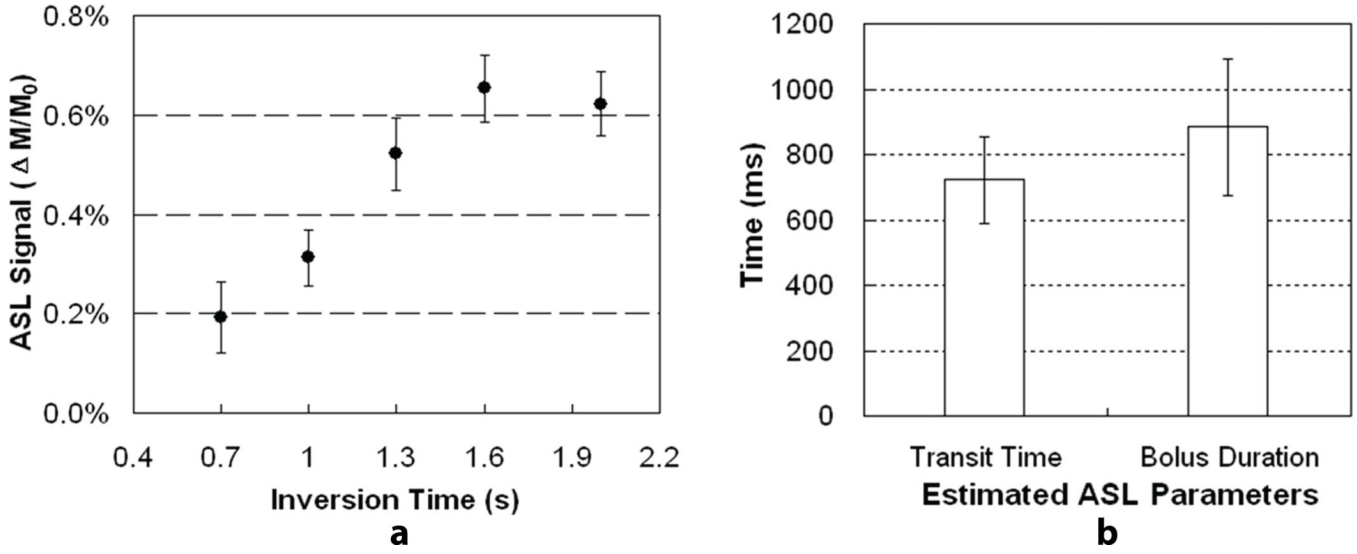

Figure 4.
Results from multiple inversion perfusion studies for all five subjects: (a) measured ASL signals as a function of inversion time after compensating for longitudinal relaxation; (b) mean and standard deviation of estimated arterial transit time and temporal bolus duration.

Table 1

Measurements of prostate blood flow (PBF) and estimated measurement errors due to random and temporal noises

Subject No.	Age (years)	Volume (cm^3)	PBF (mL/100 cm^3/min)	Random Error (mL/100 cm^3/min)	Random Error /PBF (%)	Temporal Error (mL/100 cm^3/min)	Temporal Error /PBF (%)
1	29	12.3	33.9	0.68	2.1	4.8	14.9
2	29	11.2	22.5	0.91	4.3	4.5	21.1
3	39	10.0	31.2	1.59	5.4	2.5	8.4
4	57	17.8	31.7	0.81	2.7	7.5	24.9
5	65	16.8	16.4	0.49	3.1	5.7	36.6
Mean	44	13.6	25.8	0.90	3.5	5.0	21.2
Standard Deviation	16	3.5	7.1	0.42	1.3	1.8	10.7